

Apparent Vs. True Bond Strength of Steel and PC with Nanoalumina

AlaEddin Douba^{1,a}, Moneeb Genedy^{2,b}, Edward Matteo^{3,c}, John Stormont^{4,d}
and Mahmoud Reda Taha^{5,e}

¹*Graduate Student, Dept. of Civil Eng., University of New Mexico, Albuquerque, NM, USA*

²*Member of Technical Staff, Sandia National Laboratories, Albuquerque, NM, USA*

³*Senior Member of Technical Staff, Sandia National Laboratories, Albuquerque, NM, USA*

⁴*Professor, Dept. of Civil Eng., University of New Mexico, Albuquerque, NM, USA*

⁵*Professor & Chair, Dept. of Civil Eng., University of New Mexico, Albuquerque, NM, USA*

^a douba@unm.edu , ^b moneeb@unm.edu , ^c enmatte@sandia.gov , ^d jcstorm@unm.edu , ^e mrtaha@unm.edu

Keywords: Nanomaterials, Slant Shear, Finite Element Analysis, Bond Strength.

Abstract

Bond of polymer concrete (PC) to steel surface is a critical aspect in many infrastructure applications. Bond strength can be evaluated through several means including pull-off, flexural, twist-off, and slant shear tests. While pull-off strength tests are the most common method for evaluating bond for PC overlays in bridge and parking structures, slant shear tests are more suitable when vertical rather than horizontal bond lines are used. In this paper, we discuss the use of slant shear tests to examine bond of polymer concrete repair material to steel pipes used to ensure wellbore integrity of abandoned oil wells used for CO₂ sequestration.

Bond strength of Novolac PC incorporating nanoalumina particles to steel surface was measured using slant shear test. Different amounts of nanoalumina were used in PC to improve bond strength without significantly reducing PC flowability. Slant shear testing confirmed the ability of nanoalumina to improve the steel-PC bond strength. A finite element (FE) model using ABAQUS simulation environment was developed to compare the apparent versus the true bond strength. A cohesive contact element surface was used to simulate bond along the interface line. The FE model showed stiffness mismatch between the PC and steel controls the maximum shear stress developed at the interface surface. The true bond strength extracted from the FE model appears to be about twice that of the apparent bond strength.

Introduction

Polymer concrete (PC) has been widely used in many infrastructure applications due to its attractive mechanical properties and ease of application [1]. Furthermore, PC has been successfully used as a repair material given its strong bond to existing concrete and steel substrates [2]. Integrity of abandoned oil wells has recently appeared as a critical issue that hinders the international efforts for carbon capture and storage for CO₂ sequestration [3]. It has been suggested that PC incorporating nanoparticles might be a suitable repair and seal material with its superior bond strength with the steel casing in abandoned oil wells for efficient CO₂ sequestration [4]. Nanoparticles interact with the host polymer to produce a new polymer nanocomposite with altered mechanical properties [4-5]. Carbon nanotubes (CNTs), Graphene Nanoparticles (GNPs) and Nanoalumina (NAL) were reported in the literature as potential candidate nanoparticles to alter the glass transition temperature, compressive strength, modulus of elasticity, energy absorption and durability of polymers [5-6].

Bond strength of PC against steel casing is developed by chemical and physical bonds [2,7]. Several tests are performed to evaluate the bond strength of repair materials. Pull-off, twist-off, direct tension, flexural and slant shear tests are among the most common [8]. Pull-off test often provides the most conservative bond strength and is commonly used in evaluating bond strength of PC overlay to steel bridge deck. However, slant shear test has been suggested to be more suitable to examine bond strength with vertical bond lines [9]. In a slant shear test, the PC-steel interface is subjected to combined shear and compressive stresses. The angle of the interface along with surface roughness are key parameters controlling the behavior in slant shear test [9-11]. Slant shear test is often used to examine bond strength of two different materials; the repair material and the substrate being concrete, steel or rock surface. When the two materials hold different stiffness, stiffness mismatch transpires at the interface leading to areas of stress concentration [9-10]. Therefore, the average/apparent bond strength obtained through slant shear test of two different materials does not necessarily represent the true shear strength at the interface. The use of finite element (FE) method is then essential to obtain realistic estimate of the shear stress and its distribution along the interface. This paper investigates the bond strength of PC incorporating NAL particles with steel substrate. NAL is used at different concentrations to improve the bond strength of PC and steel substrate. A comparison between apparent and true bond strength is also conducted through the integration of slant shear test observations and finite element modeling.

Experimental Methods

Materials. Novolac epoxy resin was used. Novolac epoxy is specifically designed to provide high thermal stability and chemical resistance. The hardener was Diethylenetriamine (DETA), Phenol, 4,4'-(1-methylethylidene)bis-, and Tetraethylbenzepentamine. Crystalline silica (quartz) and ceramic microspheres powder were used as mixing filler to produce the PC slurry. The nanoalumina (NAL) used is Aluminium Oxide (Al₂O₃) nanoparticles manufactured by Sigma Aldrich, Inc. and has a maximum particle size of 50 nm. The total NAL used was 0.5 wt.%, 1.0 wt.% and 2.0 wt.% of the Novolac epoxy resin by weight. PC mix proportions used are reported in Table 1.

Table 1: PC mixture proportions (kg/m³).

Mix	NAL incorporated	Epoxy resin	Epoxy Hardener	Silica particles
PC-Neat	Zero			
PC-0.5	0.5 wt.% = 1.11			
PC-1.0	1.0 wt.% = 2.21	221	96	1200
PC-2.0	2.0 wt.% = 4.42			

Specimen Preparation. Uniform dispersion of nanomaterials within the polymer matrix is criterial prior to producing PC. First, the Novolac epoxy resin was heated to 110°C. The nanomaterials were then added and left for two hours to disperse. The polymer-nanomaterials mix was magnetically steered to 800 rpm. The high temperature helps reducing the viscosity of the epoxy resin and thus improves dispersion of nanoparticles. The polymer nanocomposite was then placed in the Sonicator for two hours at 60°C. Sonication generates sound waves that creates microscopic bubbles within the heated liquid to improve dispersion. The polymer nanocomposite mix was then degased to discard all subsequent bubbles from the resin. The resin was then left to cool down to room temperature for one hour. The hardener was then added and mixed for 2-3 minutes with the resin/nanoparticles mix. The filler was then added and mixed for 3 additional minutes until the PC matrix was uniform. Five specimen were cast with two fillings each compacted 25 times and left to cure at room temperature for seven days. All tests were carried out at 7 days of age. Flowability, slant shear and compression tests to extract stress-strain relationship were performed according to ASTM specifications for different PC mixes.

Flowability Test. Flowability was performed according to ASTM C1437 [12]. A 70/100 mm diameter cone with 50 mm height was used in this test. Flowable PC was filled with two layers each compacted 20 times on the flow table. 25 strikes were applied on the flow table and four readings are obtained using the test caliber. The sum of these readings represent the flowability of the polymer concrete. Fig.1 shows the flowability test process.



Fig.1: Flowability test process: (a) Cone filling (b) Flowability reading.

Slant Shear Test. Slant shear test was performed according to ASTM C882/C882M [13]. PC was cast on top of the steel substrate that represents one half of a cylinder with a 60 degree surface. The steel surface was roughened through industrial level sand blasting to a minimum of 4.0 Mil clean. Slant shear test was carried out as shown schematically in Fig. 2. Apparent shear strength was calculated using Eq.1 where P is the vertical load and A is the cross-sectional area.

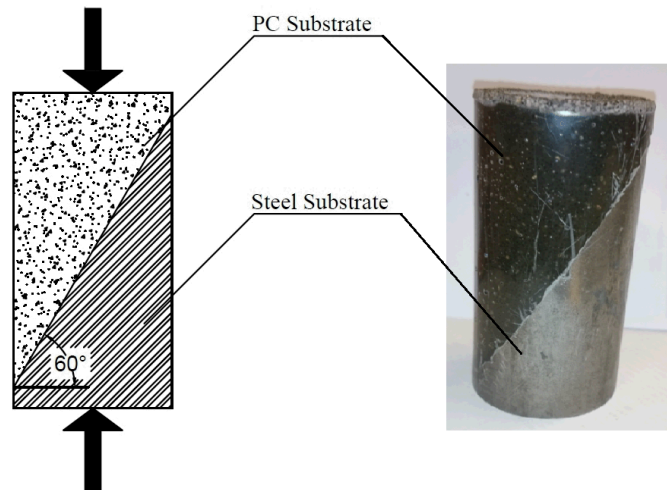


Fig. 2: Slant shear test: (a) Schematic description (b) Actual specimen.

$$\sigma = \frac{P}{A \cos(60)} \quad (1)$$

Stress-Strain Test. The constitutive stress-strain relationship of PC was performed for selected mixes using ASTM C469/C469M [14]. Vertical and horizontal strain gauges were used to measure longitudinal and lateral strains. The test allowed determining the modulus of elasticity and Poisson's ratio using Eq.2 and Eq.3 respectively. $\Delta\sigma$ is the change in stress within linear region of the stress-strain relationship. $\Delta\varepsilon_{VL}$ is the corresponding change in vertical strain and $\Delta\varepsilon_{Lat}$ is the corresponding change in lateral strain within this specific change in stress $\Delta\sigma$.

$$E = \frac{\Delta\sigma}{\Delta\varepsilon_{VL}} \quad (2)$$

$$\rho = \frac{\Delta\varepsilon_{VL}}{\Delta\varepsilon_{Lat}} \quad (3)$$

Finite Element Analysis

FE analysis was carried using ABAQUS/CAE simulation environment in order to identify true shear stress exerted at the interface during slant shear tests. PC-Neat model was used as a reference where convergence study was performed using two types of elements; 8-node linear hexagonal and 6-node linear triangular. For each element, several mesh sizes were applied in order to validate the model's convergence. Load-displacement curves extracted from the model were compared to the obtained curves from slant shear tests. PC material was defined using the constitutive stress-strain relationship determined experimentally. Steel part was assumed to be elastic perfectly plastic. The FE model constructed for slant shear is shown in Fig. 3(a).

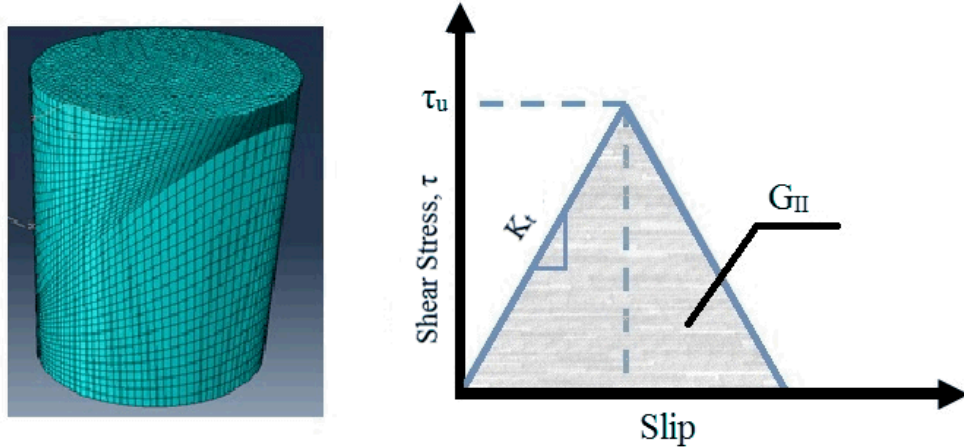


Fig. 3: FE model: (a) Slant shear model in Abaqus (b) Shear stress-slip interface relation where K_t is shear contact stiffness, G_{II} is mode II fracture energy and τ_u is maximum shear stress.

Zero-thickness contact elements were used to define the interface between PC and steel. In this element, damage and cohesive behavior were defined. The bilinear shear stress vs. slippage model is shown in Fig. 3(b) was used to define maximum shear stress, mode II fracture energy, viscosity coefficient and shear contact stiffness denoted τ_u , G_{II} , V , and K_t respectively. In this paper, the maximum shear stress (τ_u) is referred to as the true shear strength. The interface interaction parameters were back calculated to fit the load-displacement response of the experimental slant

shear test. Table 2 summarizes the contact interaction properties for all models. The FE model was executed under displacement control with boundary conditions that fix the bottom of the specimen and prevent lateral deformations. Fig. 4 shows the shear stress-shear slip relationship for PC-Near and PC-2.0 from the slant shear tests along with results of FE analysis.

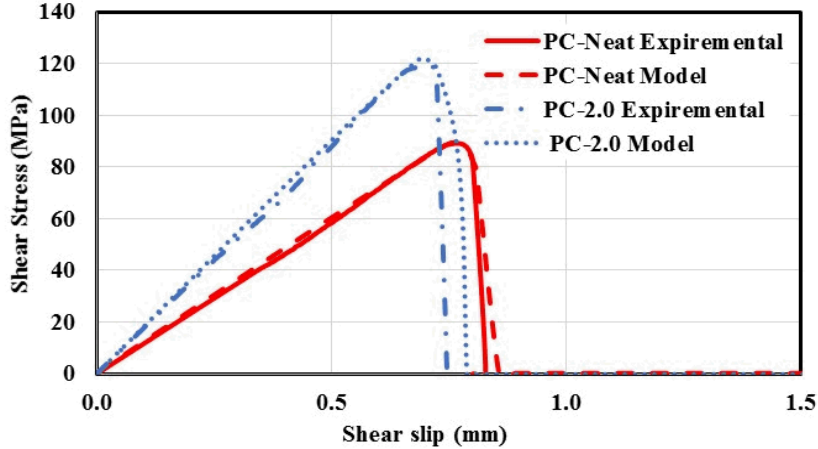


Fig. 4: Shear stress versus slip in slant shear test and FE analysis.

Table 2: Interface interaction properties defined in ABAQUS.

Contact Property	Value		PC-Neat	PC-2.0
Damage	Initiation	Maximum shear stress (τ_u), MPa	43	61
	Evolution	Fracture energy (G_{II}), N/mm	19	24
	Stabilization	Viscosity Coefficient (V)	0.001	0.001
Cohesive Behavior	Shear contact stiffness (K_t) MPa/mm		56	92

Results and Discussion

Flowability of all PC mixes was evaluated in order to better understand the effect of incorporating nanomaterials at different percentages. Fig. 5 shows the results for all PC mixes. The addition of nanoparticles to the epoxy matrix decreased the flowability to an extent. The test results also show higher concentrations of NAL to further lower flowability. However, it is important to note that a reduction in flowability within 14-16% is insignificant and thus does not have much impact on fabrication of PC.

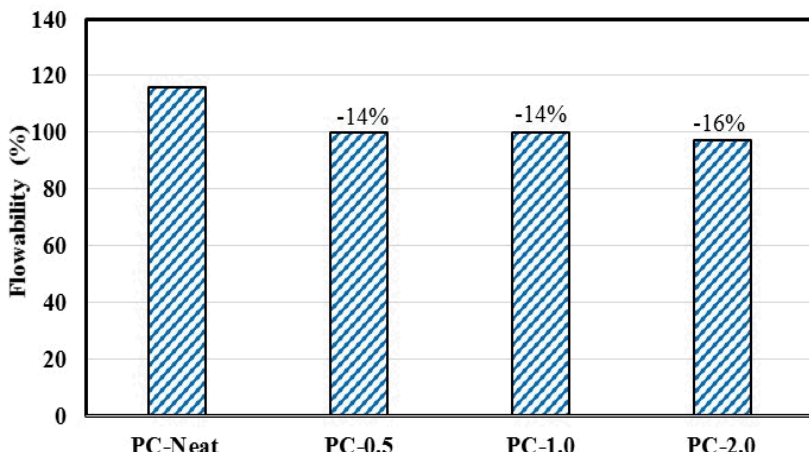


Fig. 5: Flowability test results.

Fig.6 shows the results of apparent shear/bond strength as determined using the slant shear test and Eq. 1. Incorporating 0.5, 1.0 and 2.0 wt.% NAL within the epoxy resin corresponds to an increase in the apparent bond strength of 20, 23 and 51% respectively. The increase in the apparent bond strength might be attributed to the chemical reaction of the NAL particles and the OH group that is formed on the steel surface during sand blasting [15]. PC-2.0 showed the highest increase in bond strength of 51% compared with PC-Neat. It is apparent that the use of high NAL content (2.0 or above) can increase the bond strength significantly. However, high content of NAL would jeopardize the flowability of PC limiting its applications as repair material. A maximum NAL content of 2.0% might be recommended for repair of abandoned oil well.

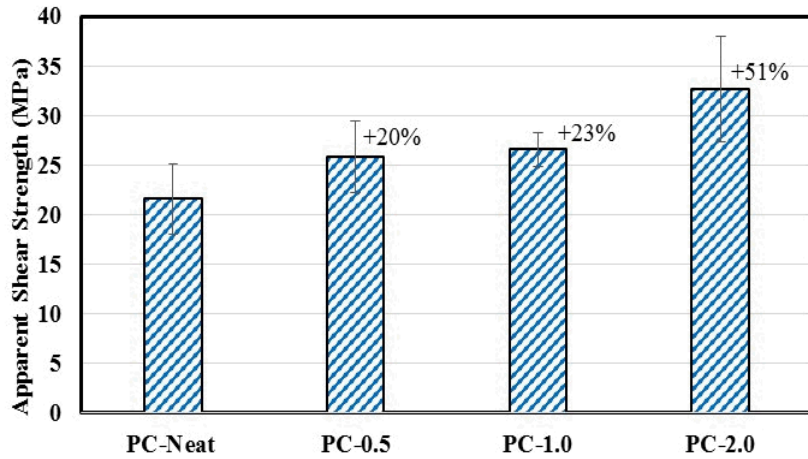


Fig. 6: Apparent shear strength for different NAL content as determined by slant shear test.

Considering the two materials in the slant shear test; steel and PC, there is significant stiffness mismatch at interface. Hence, the simple method of calculating apparent shear strength is insufficient as it does not take the significance of stiffness mismatch into account. High stiffness mismatch can lead to high stress concentrations at the interface. Shear stresses higher than the apparent shear strength might take place. Fig. 7 shows the stress-strain relation for PC-Neat and PC-2.0 as determined experimentally. PC incorporating 2.0 wt.% NAL has a stiffness that is 12% higher than neat PC. Increasing PC stiffness decreases the stiffness mismatch and hence results in lowering the difference between the apparent and the true shear strength. Nonetheless, it is important to note that Poisson's ratio of PC is also altered by incorporating nanoparticles. Experimental observations in the stress-strain test showed an increase in Poisson's ratio by 42% when 2.0 wt.% NAL are incorporated in the PC mix. An increase in Poisson's ratio corresponds to reducing the stresses at the interface.

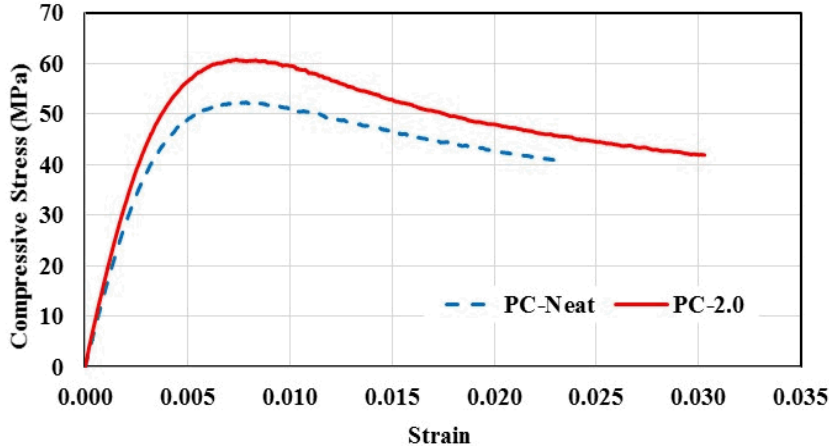


Fig. 7: Stress-strain relationship for PC-Neat and PC-2.0 as determined experimentally.

Further investigation on bond strength was carried using FE method. By modeling slant shear tests to include material's stiffness, the true bond strength (i.e. the maximum shear stress necessary to achieve the slant shear behavior) of PC-Steel was determined. Fig. 8 shows the true bond strength as calculated using the FE method vs. the apparent bond strength from slant shear test. It is obvious that that a significant difference between the apparent and the true bond strength can be observed. PC-Neat and PC-2.0 showed 99% and 87% increase in true bond strength compared to the apparent bond strength respectively. It is interesting to note the reduction in the difference between the true and apparent bond strength from 99% of PC-Neat to 87% of PC-2.0. This reduction is attributed to the observed effect of NAL to increase the modulus of elasticity of PC and thus reducing the stiffness mismatch between PC and steel at the interface. Apparently, the effect of stiffness mismatch manipulates the shear stress at the interface when testing two different materials using slant shear method. The apparent bond strength does not realistically reflect the true bond strength when significant stiffness mismatch between the two halves of the slant shear test exists.

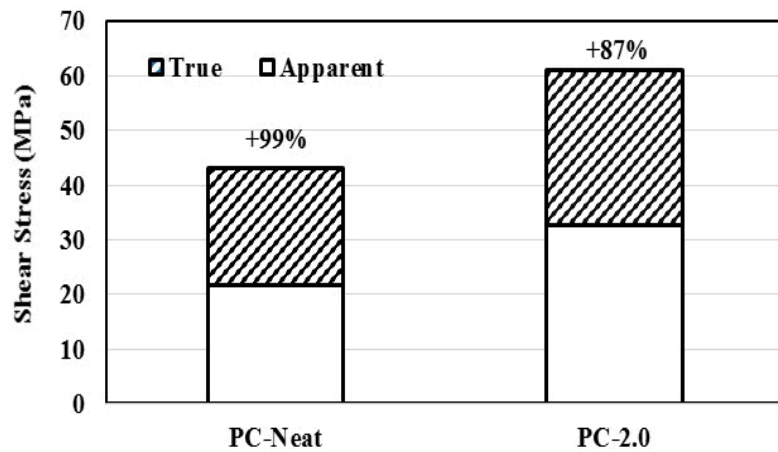


Fig. 8: True vs. apparent shear strength of PC as determined experimentally and using FE method.

Finally, the developed FE model can shed light on the location of the maximum shear stress along the interface. Fig. 9 shows shear contours at the PC-Neat interface at selected slippage points for vertical displacement specifically at (a) 0.720mm, (b) 0.802mm and (c) 0.837mm. Those points are also shown on the load-displacement curve in Fig. 10. Snapshots of the FE model with magnified slippage are tied to the load-displacement curve for pictorial description. The maximum shear stress (τ_u) (i.e. true bond strength) was obtained at various locations on the surface. During

initial slippage, locations of stress concentration are skewed towards minimum volume of PC. As slippage continue, condensed regions of stress concentration shift along the interface. The pathway of stress concentration localities follows slippage and is directly related to the volume of PC. The development process of stresses confirms the significant of stiffness mismatch on PC-Steel interface.

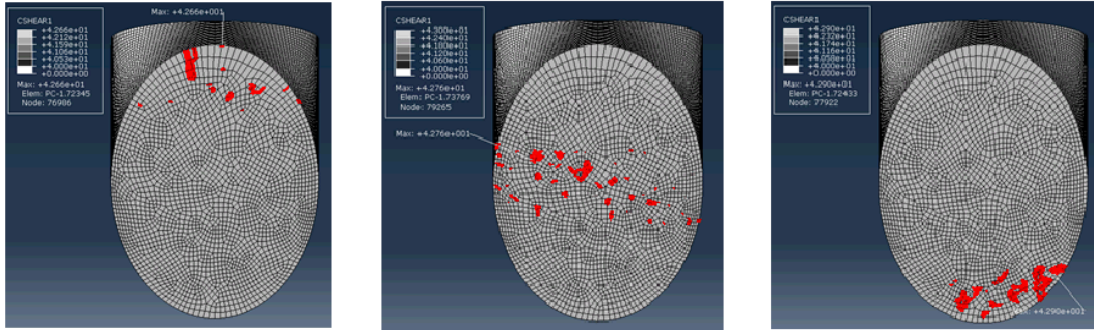


Fig. 9: Shear contours at PC-Neat interface for three vertical displacements of
(a) 0.720mm, (b) 0.802mm and (c) 0.837mm.

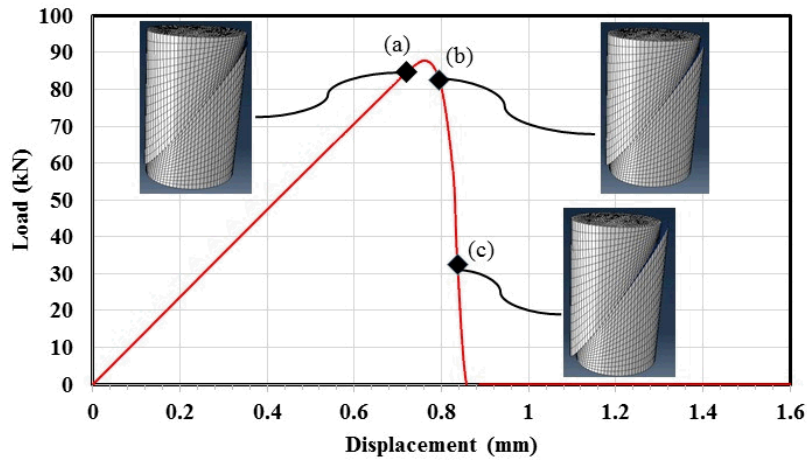


Fig. 10: Load-displacement of PC-Neat showing slippage at different vertical displacements
(a) 0.720mm, (b) 0.802mm and (c) 0.837mm.

Conclusion

Our experimental investigation showed NAL tends to slightly hinder the flowability of the matrix. The reduction in flowability for NAL concentrations of up to 2.0 wt.% of the epoxy resin was insignificant. It is evident that nanoalumina particles improve the bond strength of PC to steel surfaces. Using slant shear test showed that NAL concentrations of up to 2.0 wt.% of the epoxy resin was able to improve the apparent (average) bond strength by to 51%. Stress-strain curves determined experimentally showed that addition of NAL also increased the stiffness as well as Poisson's ratio of PC compared with neat PC. Further investigation was carried using the finite element method proved that there is a significant difference between the apparent bond strength and the true bond strength represented by the maximum shear stress occurring at the interface. The true bond strength is about twice the apparent one. This was attributed to the significant stiffness mismatch between PC and steel. Increase the NAL concentrations, increased PC stiffness and slightly reduced the stiffness mismatch. The maximum local shear stress occurred at the interface area with the minimum PC volume and moved along the interface as shear slippage took place.

Acknowledgement

This material is based upon work supported by the U.S. Department of Energy (DOE) National Energy Technology Laboratory (NETL) under Grant Number DEFE0009562. This project is managed and administered by the DOE/NETL Storage Division and funded by DOE/NETL and cost-sharing partners. This paper was prepared as an account of work sponsored by an agency of the United States Government. Neither the United States Government nor any agency thereof, nor any of their employees, makes any warranty, express or implied, or assumes any legal liability or responsibility for the accuracy, completeness, or usefulness of any information, apparatus, product, or process disclosed, or represents that its use would not infringe privately owned rights. Reference herein to any specific commercial product, process, or service by trade name, trademark, manufacturer, or otherwise does not necessarily constitute or imply its endorsement, recommendation, or favoring by the United States Government or any agency thereof. The views and opinions of authors expressed herein do not necessarily state or reflect those of the United States Government or any agency thereof.

Sandia National Laboratories is a multi-program laboratory managed and operated by Sandia Corporation, a wholly owned subsidiary of Lockheed Martin Corporation, for the U.S. Department of Energy's National Nuclear Security Administration under contract DE-AC04-94AL85000. SAND2014-16879 CCN infuse the properties of nanoparticles with the host epoxy resin acquiring improved mechanical properties. This investigation aimed to examine the bond strength of PC incorporating NAL with steel through slant shear test. The main application for this research is to ensure proper sealing of abounded oil wells for CO2 waste storage.

References

- [1] ACI Committee 548, *Polymers and Adhesives in Concrete*, State of the Art Report, 2009.
- [2] C. Vipulanandan & E. Paul. Characterization of Polyester Polymer and Polymer Concrete. *Journal of Materials in Civil Engineering*. 1993; 5, 1, 62-82.
- [3] M. Zhang & S. Bachu. Review of integrity of existing wells in relation to CO2 geological storage: What do we know? *International Journal of Greenhouse Gas Control*. 2011; 5, 4, 826-840.
- [4] M. Genedy, J. Stormont, E. Matteo and M. Reda Taha. Examining epoxy-based nanocomposites in wellbore seal repair for effective CO₂ sequestration. *Energy Procedia*. 2014; 63, 3, 5798-5807.
- [5] B. Wetzel, P. Rosso, F. Haupert, & K. Friedrich. Epoxy nanocomposites - fracture and toughening mechanisms. *Engineering Fracture Mechanics*. 2006; 73, 2375-2398.
- [6] N. Salemi & K. Behfarnia. Effect of nano-particles on durability of fiber-reinforced concrete pavement. *Construction and Building Materials*. 2013; 48, 1, 934-941.
- [7] A. Baldan Adhesively-bonded joints and repairs in metallic alloys, polymers and composite materials: Adhesives, adhesion theories and surface pretreatment. *Journal of Materials Science*. 2004; 39(1):1-49.
- [8] A. Momayez, M. R. Ehsani, A. A. Ramezanianpour & H. Rajaie. Comparison of methods for evaluating bond strength between concrete substrate and repair materials. *Cement and Concrete Research*. 2005; 35, 4, 748.
- [9] M. Naderi. Analysis of the slant shear test. *Journal of Adhesion Science and Technology*. 2009; 23, 2, 229-245.

[10]S. Austin, P. Robins & Y. Pan. Shear bond testing of concrete repairs. *Cement and Concrete Research*. 1999; 29, 7, 1067.

[11]R. Saldanha, E. Julio, D. Dias-da-Costa & P. Santos. A modified slant shear test designed to enforce adhesive failure. *Construction and Building Materials*. 2013; 41, 673-680.

[12]ASTM C1437-13. Standard test method for flow of hydraulic cement mortar. *ASTM International*, West Conshohocken, PA. 2013.

[13]ASTM C882/C882M-13a. Standard test method for bond strength of epoxy-resin systems used with concrete by slant shear. *ASTM International*, West Conshohocken, PA. 2013.

[14]ASTM C469/C469M. Standard test method for static modulus of elasticity and Poisson's ratio of concrete in compression. *ASTM International*, West Conshohocken, PA. 2014.

[15] A. V. Pocius, *Adhesion and Adhesives Technology: An Introduction*. 2nd ed. Munich: Hanser; 2011.